

Click Chemistry

DOI: 10.1002/anie.201301930

## Plasmon Resonance Scattering Spectroscopy at the Single-Nanoparticle Level: Real-Time Monitoring of a Click Reaction\*\*

Lei Shi, Chao Jing, Wei Ma, Da-Wei Li, Jonathan E. Halls, Frank Marken, and Yi-Tao Long\*

Understanding and monitoring chemical reactions is crucial for the characterization of reaction mechanisms in organic chemistry. Various analytical methods including nuclear magnetic resonance spectroscopy,[1] mass spectrometry,[2] and Raman spectroscopy<sup>[3]</sup> have been employed to study chemical reactions. For example, the oxidation of carbon monoxide on gold catalyst surfaces was studied using timeresolved IR spectroscopy.<sup>[4]</sup> However, the averaged signals obtained from multiple nanoparticles cannot provide as accurate information on the nanoscale level compared to the signals obtained from a single nanoparticle.<sup>[5]</sup> Differences in size and shape are unavoidable in nanoparticle production, and such differences cannot be distinguished by averaged measurements. Moreover, nanoparticles with different size and shape exhibit different physical and chemical properties, including spectral bands, reaction activity, and efficiency. Measurements from single nanoparticles could reveal the unique function of individual particles, and thus be superior to the averaged measurements taken from bulk solutions. Notably, every single nanoparticle could serve as an independent sensor and provide significant signals with high signal-to-noise ratio, [6] which dramatically lowers the detection limit and enables higher spatial and temporal resolution. For example, single gold nanoparticles (GNPs) could be used to detect single unlabled proteins.<sup>[7]</sup>

The advent of plasmon resonance Rayleigh scattering (PRRS) spectroscopy and dark-field microscopy (DFM) has helped the study of the size, shape, composition, and the local environment of single plasmonic nanoparticles.<sup>[8]</sup> DFM is a highly sensitive direct means to probe chemical analytes.<sup>[8a,9]</sup> However, the application of DFM to monitor chemical reactions is rare.<sup>[10]</sup> To observe the behavior of nanoparticles during reactions, it is essential to monitor the spectra of

nanoparticles at the single-particle level. When multiple plasmonic nanoparticles are in close proximity, it is worthy to note that their plasmonic oscillations can couple together, resulting in a large increase in light-scattering intensity as well as a spectral red-shift and the obvious color changes observed in DFM.<sup>[11]</sup> This phenomenon has been used to construct plasmon rulers.<sup>[12]</sup> For example, when two gold nanoparticles were linked by DNA, the intensity would increase by 44 times and the wavelength would red-shift by 75 nm compared with an individual nanoparticle.<sup>[13]</sup>

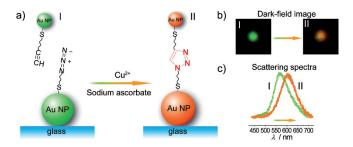
Click chemistry is a powerful, highly reliable and selective method in synthesis chemistry. [14] Cu<sup>+</sup>-catalyzed azide–alkyne 1,3-dipolar cycloaddition (CuAAC) is considered as a typical click reaction with very high yields and good regioselectivity, and has attracted widespread interest. To date, it has been widely applied in polymer and material science, [15] drug discovery, [16] biochemistry, [17] pharmaceutical science, [18] and also used to functionalize the surface of nanoparticles (Au, Ag) to construct sensors. [19]

Herein, we describe a novel method to monitor a Cu<sup>+</sup>-catalyzed click reaction at the single-nanoparticle level by using PRRS spectroscopy and DFM. Click reactions result in interparticle cross-linking, which induces a color change of GNPs in DFM and a scattering spectral red-shift. To the best of our knowledge, this is the first time that a click reaction has been monitored at the single-nanoparticle level, thus making this method a valuable technique for the real-time monitoring of chemical reactions in organic chemistry.

Our strategy is shown in Scheme 1. We synthesized terminal azide- and alkyne-functionalized thiols and prepared the system shown through the following steps (see the Supporting Information for more details): 1) immobilization of 60 nm GNPs on a cleaned ITO (indium tin oxide) glass slide; 2) self-assembly of the azide-functionalized thiol on the

[\*] L. Shi, [\*] C. Jing, [\*] Dr. W. Ma, Dr. D.-W. Li, Prof. Y.-T. Long State Key Laboratory of Bioreactor Engineering Shanghai Key Laboratory of Functional Materials Chemistry & Department of Chemistry
East China University of Science and Technology Shanghai, 200237 (P. R. China)
E-mail: ytlong@ecust.edu.cn
J. E. Halls, Prof. F. Marken
Department of Chemistry, University of Bath Claverton Down, Bath BA2 7AY (UK)

- [+] These authors contributed equally to this work.
- [\*\*] This research was supported by the 973 Program (2013CB733700), the National Science Fund for Distinguished Young Scholars (21125522), and the National Natural Science Foundation of China (91027035).
- Supporting information for this article is available on the WWW under http://dx.doi.org/10.1002/anie.201301930.



**Scheme 1.** a)  $Cu^+$ -catalyzed click reaction at the single-particle level. b) A typical dark-field image of a modified GNP on a microscopy slide before (I) and after (II) the addition of  $Cu^{2+}$  and sodium ascorbate. c) Corresponding scattering spectra of a single GNP before (I) and after (II) the click reaction.



surface of the 60 nm GNPs; 3) self-assembly of the alkynefunctionalized thiol on the surface of 14 nm GNPs; 4) addition of modified 14 nm GNPs onto the modified ITO glass side. The 60 nm and 14 nm GNPs were characterized by UV/ Vis spectra and SEM (see the Supporting Information, Figure S1). In this assay, the 14 nm GNPs were linked to a 60 nm GNPs by click chemistry (Scheme 1a). The Cu<sup>+</sup> is obtained from the reduction of Cu<sup>2+</sup> in the presence of sodium ascorbate.

To investigate the feasibility of this method, dark-field color images of single GNPs and PRRS spectra  $\lambda_{max}$  were used to probe the Cu<sup>+</sup>-catalyzed click reaction. Compared with the scattering spectra in the absence of Cu<sup>2+</sup> and sodium ascorbate, the scattering spectra exhibit an obvious peak red-shift after the introduction of Cu<sup>2+</sup> and sodium ascorbate. Time-dependent  $\Delta\lambda_{max}$  changes of a selected single gold nanoparticle are shown in Figure 1a. A single gold nanoparticle with green color in the DFM image has a scattering peak centered at 560 nm. After the addition of Cu<sup>2+</sup> and sodium ascorbate, the scattering peak ( $\Delta\lambda_{max}$ ) red-shifted to increasingly longer wavelengths, and the green spots in DFM images gradually changed to orange (inset of Figure 1a).

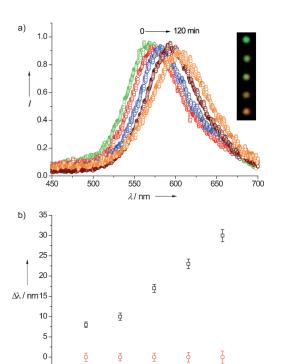


**Figure 1.** a) Representative scattering spectra of single azide-functionalized GNPs (60 nm) obtained at different times after treatment with Cu<sup>2+</sup> (1 μm), sodium ascorbate (10 μm), and alkyne-functionalized GNPs (14 nm), showing that the  $\lambda_{max}$  of the PRRS spectra is red shifted. Inset: Corresponding dark-field images of individual nanoparticles after treatment with Cu<sup>2+</sup> and sodium ascorbate, showing a color change from green (control) to orange (120 min). b) Plots of the peak shift for a single azide-functionalized GNP (60 nm) in the presence (square) and absence (circle) of sodium ascorbate after 30 min in the presence of Cu<sup>2+</sup> (0.1 nm to 1 μm) and alkyne-functionalized GNPs (14 nm).

[Cu<sup>2+</sup>] / M

 $\Delta\lambda_{max}$  of up to 43 nm were observed upon interparticle coupling after 2 h. The results demonstrate that the scattering-peak wavelength of the interacting particles is red-shifted from that of a single particle, because of near-field coupling by the click reaction; this finding was further confirmed by scanning-electron microscope images (see the Supporting Information, Figure S2). The red-shifting with time, in the spectra of the GNP, may be attributed to the inhomogeneous diffusion of  $Cu^{2+}$  ions and the diffusion of 14 nm GNPs.

As  $Cu^+$  is the catalyst, its concentration was important for the reaction. We measured the  $\Delta \lambda_{max}$  at different concentrations of  $Cu^{2+}$  after 30 min. Single GNPs giving an initial scattering peak around 560 nm were chosen to test the influence of changing the concentration of  $Cu^{2+}$ . We added an aqueous solution of  $Cu^{2+}$  to the solution on the ITO glass slide to obtain  $Cu^{2+}$  concentrations of 0.01 nm, 0.1 nm, 1 nm, 10 nm, 100 nm, and 1  $\mu$ m. Sodium ascorbate was also added at five times the concentration of  $Cu^{2+}$ . As shown in Figure 1 b,  $\Delta \lambda_{max}$  increased with the increasing concentration of  $Cu^{2+}$ . However, no corresponding increase in  $\Delta \lambda_{max}$  was seen in the absence of sodium ascorbate. Within the same reaction time, the minimum detectable catalyst concentration of  $Cu^{2+}$  was 0.1 nm.

To prove that this method cannot only be used for individual particles, we presented a larger visual field showing the color changes of all particles, from the bulk solution, after coupling in 1.5 h. Figure 2a and c show the dark-field images of about 900 individual GNPs. Results indicate that the color of the nanoparticles changed from green to orange upon the interparticle coupling in the presence of Cu<sup>2+</sup> and sodium ascorbate. In addition, the peak wavelength  $(\lambda_{max})$  of the GNPs was calculated from the RGB (red, green, and blue) information of the color images by using Matlab. [8c] Figure 3b and d show the calculated peak wavelength of GNPs at 560  $\pm$ 10 nm before coupling (b) and  $580 \pm 10$  nm after coupling (d). The calculated statistic data of numerous nanoparticles indicates that the method is highly reproducible and reliable. SEM images of a larger number of assembled nanoparticles after the click reaction are shown in the Supporting Informa-

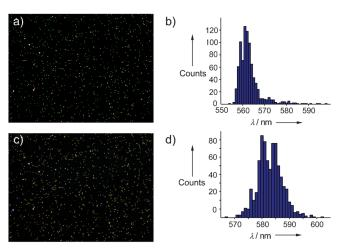


**Figure 2.** Dark-field images and calculated wavelength of the GNPs (60 nm) before (a and b, respectively) and after (c and d, respectively) the addition of  $Cu^{2+}$  (1 μm) and excess sodium ascorbate.

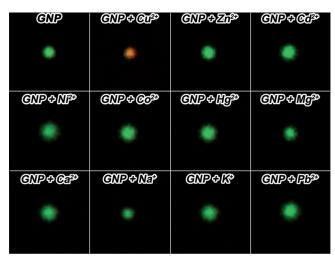


Figure 3. Dark-field images of single gold nanoparticles (60 nm diameter) in the presence of different metal ions.

tion, Figure S3. From the SEM images we can see that the binding events are different for every 60 nm nanoparticle. Thus, the signals obtained from the detection of single particles reveal the differences between every individual particle, unlike averaged signals obtained from bulk solutions.[19]

We also measured the color changes in DFM and the scattering spectra in the presence of representative coexisting ions, including Zn<sup>2+</sup>, Cd<sup>2+</sup>, Ni<sup>2+</sup>, Co<sup>2+</sup>, Hg<sup>2+</sup>, Mg<sup>2+</sup>, Ca<sup>2+</sup>, Pb<sup>2+</sup>, Na<sup>+</sup> and K<sup>+</sup>, (Figure 3). Remarkably, upon introduction of these metal ions and sodium ascorbate, neither color change nor spectral peak shift was observed even at much higher concentration (1 µm). Only the presence of Cu<sup>2+</sup> and sodium ascorbate could induce the coupling of the GNPs. Also, no color change was observed in control experiments with nanoparticles in the absence of Cu<sup>2+</sup> or sodium ascorbate or both, thus confirming that the coupling was mediated by Cu<sup>2+</sup> and sodium ascorbate. These results further confirm that catalysis of the click reaction is specific to Cu<sup>2+</sup> (reduced to Cu<sup>+</sup> by sodium ascorbate). Sensors based on gold nanoparticles also have been applied to detect heavy-metal ions.<sup>[20]</sup> Our system could be used to probe Cu<sup>2+</sup> with high sensitivity (the minimum detectable concentration is 0.1 nm) and high selectivity.

In conclusion, we developed a novel method for real-time monitoring of the click reaction by using PRRS spectroscopy and DFM at single-nanoparticle level. The method involves the interparticle coupling by CuAAC. The click reaction on the surface of single GNPs resulted in interparticle coupling leading to a red-shift of PRRS spectra and a color change in DFM. Furthermore, our studies demonstrated the ability to use DFM and scattering spectra to investigate the reaction time and the amount of catalyst. We believe that our strategy could play an important role in the monitoring of chemistry reactions, especially coupling reactions, in organic chemistry. Accordingly, future efforts will be directed to characterize other chemical reactions by using single plasmonic nanoparticles.

## Experimental Section

Synthesis and characterization of gold nanoparticles: GNPs with average diameters of 14 nm were prepared by the citrate-mediated reduction of HAuCl<sub>4</sub>. HAuCl<sub>4</sub> (0.01 wt %; 50 mL) was heated to reflux with vigorous stirring and then 5 mL sodium citrate (38.8 mm) was added quickly to the solution. The solution was heated for 15 min, then the heating was stopped and the solution was stirred for an additional 15 min. Colloidal particles were filtered from the resulting suspension and characterized by an absorption maximum at 518 nm by using UV/Vis spectrometry. These particles were then used as seed particles for the synthesis of the 60 nm gold particles. Preformed seed gold particles (1 mL) and NH<sub>2</sub>OH·HCl (0.2 m; 100 μL) was added to water (25 mL). The mixture was stirred vigorously at room temperature and 3.0 mL of 0.1 wt % HAuCl<sub>4</sub>·3 H<sub>2</sub>O was added dropwise.

Single nanoparticle DFM imaging and scattering spectroscopy: The dark-field spectrum measurements were carried out on an inverted microscope (eclipse Ti-U, Nikon, Japan) equipped with a dark-field condenser (0.8 < NA < 0.95) and a  $40 \times$  objective lens (NA = 0.8). A 100 W halogen lamp provides white light to excite the GNPs and to generate plasmon resonance scattering light. The darkfield color images were captured by using a true-color digital camera (Nikon DS-fi). The scattering light of the gold nanoparticle was split by a monochromator (Acton SP2300i) equipped with a grating (grating density: 300 L mm<sup>-1</sup>; blazed wavelength: 500 nm) and recorded by a spectrometer CCD (CASCADE 512B, Roper Scientific, PI) to obtain the scattering spectra. The GNP functionalized slides were immobilized on a platform. At first, the scattering light of a single nanoparticle modified with an azide-functionalized thiol was captured in tBuOH/H2O (1:1) solution as the initial spectral wavelength. Then, the 50 % v/v  $t\mathrm{BuOH}$  solution was by pipette and 14 nm gold nanoparticles modified with an alkyne-functionalized thiol-(50 μL), CuSO<sub>4</sub> solution (1 μM), and sodium ascorbate solution (10 μM) were added to the slide. The time-dependent scattering spectra of the single nanoparticle were obtained to continuously monitor the click reaction. The scattering spectra from the individual nanoparticles were corrected by subtracting the background spectra (in absence the GNPs) taken from the adjacent regions and dividing with the calibrated response curve of the entire optical system. The spectra were integrated over 10 second.

The synthesis of the azide- and alkyne-functionalized thiols, modification procedure, characterization of the compounds and nanoparticles were performed as described in the Supporting Information.

Received: March 7, 2013 Published online: April 24, 2013

**Keywords:** click chemistry · dark-field microscopy · nanoparticles · plasmon resonance scattering spectroscopy · reaction monitoring

6013

<sup>[1]</sup> a) M. Hunger, M. Seiler, T. Horvath, Catal. Lett. 1999, 57, 199-204; b) M. V. Gomez, H. H. J. Verputten, A. Diaz-Ortiz, A. Moreno, A. de La Hoz, A. H. Velders, Chem. Commun. 2010, 46, 4514-4516; c) A. Mix, P. Jutzi, B. Rummel, K. Hagedorn, Organometallics 2010, 29, 442-447.

<sup>[2]</sup> a) X. Ma, S. Zhang, Z. Lin, Y. Liu, Z. Xing, C. Yang, X. Zhang, Analyst 2009, 134, 1863-1867; b) C.-H. Hsieh, C.-S. Chao, K.-K. T. Mong, Y.-C. Chen, J. Mass Spectrom. 2012, 47, 586-590; c) E. D. Lee, W. Mueck, J. D. Henion, T. R. Covey, J. Am. Chem. Soc. **1989**, 111, 4600 – 4604.

<sup>[3]</sup> a) T. Kobayashi, T. Saito, H. Ohtani, Nature 2001, 414, 531 – 534; b) T. M. Barnard, N. E. Leadbeater, Chem. Commun. 2006, 3615 - 3616.



- [4] J. C. Fierro-Gonzalez, B. C. Gates, Catal. Today 2007, 122, 201 210.
- [5] a) T. Klar, M. Perner, S. Grosse, G. von Plessen, W. Spirkl, J. Feldmann, *Phys. Rev. Lett.* **1998**, 80, 4249–4252; b) Y. Choi, Y. Park, T. Kang, L. P. Lee, *Nat. Nanotechnol.* **2009**, 4, 742–746.
- [6] a) A. D. McFarland, R. P. Van Duyne, *Nano Lett.* 2003, 3, 1057–1062; b) S. Berciaud, L. Cognet, P. Tamarat, B. Lounis, *Nano Lett.* 2005, 5, 515–518; c) C. Cao, S. J. Sim, *Lab Chip* 2009, 9, 1836–1839.
- [7] I. Ament, J. Prasad, A. Henkel, S. Schmachtel, C. Sönnichsen, Nano Lett. 2012, 12, 1092–1095.
- [8] a) J. Yguerabide, E. E. Yguerabide, Anal. Biochem. 1998, 262, 157-176; b) L. Zhang, Y. Li, D.-W. Li, C. Jing, X. Chen, M. Lv, Q. Huang, Y.-T. Long, I. Willner, Angew. Chem. 2011, 123, 6921-6924; Angew. Chem. Int. Ed. 2011, 50, 6789-6792; c) C. Jing, Z. Gu, Y.-L. Ying, D.-W. Li, L. Zhang, Y.-T. Long, Anal. Chem. 2012, 84, 4284-4291.
- [9] a) W.-G. Qu, B. Deng, S.-L. Zhong, H.-Y. Shi, S.-S. Wang, A.-W. Xu, *Chem. Commun.* 2011, 47, 1237; b) G. Raschke, S. Kowarik, T. Franzl, C. Sönnichsen, T. A. Klar, J. Feldmann, A. Nichtl, K. Kürzinger, *Nano Lett.* 2003, 3, 935–938.
- [10] C. Novo, A. M. Funston, P. Mulvaney, Nat. Nanotechnol. 2008, 3, 598–602.
- [11] a) A. P. Alivisatos, K. P. Johnsson, X. Peng, T. E. Wilson, C. J. Loweth, M. P. Bruchez, P. G. Schultz, *Nature* 1996, 382, 609 611;
  b) C. A. Mirkin, R. L. Letsinger, R. C. Mucic, J. J. Storhoff, *Nature* 1996, 382, 607 609;
  c) N. Liu, M. Hentschel, T. Weiss, A. P. Alivisatos, H. Giessen, *Science* 2011, 332, 1407 1410.

- [12] C. Sönnichsen, B. M. Reinhard, J. Liphardt, A. P. Alivisatos, *Nat. Biotechnol.* **2005**, *23*, 741 745.
- [13] Y.-W. Jun, S. Sheikholeslami, D. R. Hostetter, C. Tajon, C. S. Craik, A. P. Alivisatos, *Proc. Natl. Acad. Sci. USA* 2009, 106, 17735–17740.
- [14] H. C. Kolb, M. G. Finn, K. B. Sharpless, Angew. Chem. 2001, 113, 2056–2075; Angew. Chem. Int. Ed. 2001, 40, 2004–2021.
- [15] B. Helms, J. L. Mynar, C. J. Hawker, J. M. J. Fréchet, J. Am. Chem. Soc. 2004, 126, 15020 – 15021.
- [16] H. C. Kolb, K. B. Sharpless, Drug Discovery Today 2003, 8, 1128–1137.
- [17] a) P. M. E. Gramlich, C. T. Wirges, A. Manetto, T. Carell, Angew. Chem. 2008, 120, 8478-8487; Angew. Chem. Int. Ed. 2008, 47, 8350-8358; b) Y. L. Angell, K. Burgess, Chem. Soc. Rev. 2007, 36, 1674-1689.
- [18] G. C. Tron, T. Pirali, R. A. Billington, P. L. Canonico, G. Sorba, A. A. Genazzani, Med. Res. Rev. 2008, 28, 278-308.
- [19] Y. Zhou, S. Wang, K. Zhang, X. Jiang, Angew. Chem. 2008, 120, 7564–7566; Angew. Chem. Int. Ed. 2008, 47, 7454–7456.
- [20] a) X. He, H. Liu, Y. Li, S. Wang, N. Wang, J. Xiao, X. Xu, D. Zhu, Adv. Mater. 2005, 17, 2811–2815; b) C.-C. Huang, H.-T. Chang, Anal. Chem. 2006, 78, 8332–8338; c) J. Chen, A. Zheng, A. Chen, Y. Gao, C. He, X. Kai, G. Wu, Y. Chen, Anal. Chim. Acta 2007, 599, 134–142; d) A. Zheng, J. Chen, G. Wu, H. Wei, C. He, X. Kai, G. Wu, Y. Chen, Microchim. Acta 2009, 164, 17–27; e) H. Wang, Y. Wang, J. Jin, R. Yang, Anal. Chem. 2008, 80, 9021–9028.